ISSN 0967-0912, Steel in Translation, 2019, Vol. 49, No. 1, pp. 7–12. © Allerton Press, Inc., 2019.
Russian Text © S.P. Eron'ko, S.M. Garbatyuk, M.Yu. Tkachev, E.V. Oshovskaya, 2019, published in Izvestiya Vysshikh Uchebnykh Zavedenii, Chernaya Metallurgiya, 2019, No. 1, pp. 34–41.

Improving the Gas-Exhaust System at Foundry Electrofurnaces

S. P. Eron'ko[a, *], S. M. Garbatyuk[b, **], M. Yu. Tkachev[a, *], and E. V. Oshovskaya[a, ****]**

[a] *Donetsk National Technical University, Donetsk, Ukrain*
[b] *Moscow Institute of Steel and Alloys, Moscow, Russia*
**e-mail: ersp@meta.ua*
***e-mail: sgor02@mail.ru*
****e-mail: mishel-tkachev@ya.ru*
*****e-mail: evo2008@bk.ru*

Received December 10, 2018; revised December 14, 2018; accepted December 22, 2018

Abstract—Inspection of the gas-exhaust system at arc furnaces of capacity 3–10 t in the casting shops of manufacturing enterprises reveals problems responsible for copious gas and dust emissions in the production buildings, with degradation of the air quality. This is mainly associated with structural shortcomings of the systems for gas and dust evacuation from the furnace chamber through the exhaust channel, working window, and gaps between the housing and roof and also between the edges of the holes in the upper section and the electrodes within the holes. In particular, the moving joints between the rotary hoods and the gas-exhaust lines in such systems do not ensure reliable sealing. Accordingly, an improved design of the hood-rotation mechanisms has been proposed, with two sand barriers preventing the atmospheric emission of harmful emissions between the moving components. In the design of an industrial prototype, a method is developed for calculating the energy parameters of the drive in the improved system. A 1:10 scale model of the system is built to check the design and the theoretical equations. By means of a measuring system consisting of a tensoresistive converter, an ac amplifier, an analog–digital converter, and a computer, the load on the model's drive on switching from the working position to the rest position and back is determined, for two cases: with and without sand barriers to seal the mobile components. The drag in the two sand barriers on rotation of the moving element amounts to 20–26% of the total load on the drive, depending on the angular velocity of the cantilever with the hood. According to the theoretical formulas, this figure is 17–23% for hood-rotation mechanisms in arc furnaces of capacity 3–10 t. Video recordings of the smoke fluxes from the model through the gaps between its housing and the roof during simulations of steel production confirm the reliability of the sand barriers, which ensure complete sealing of joints in the hood-rotation mechanism. Practical use of the proposed design improves gas–dust evacuation from the working zone of smelting furnaces used in the foundry.

Keywords: arc furnace, gas-exhaust system, sand barriers, physical model, drive, drag torque, atmospheric emissions, air quality

DOI: 10.3103/S0967091219010066

In the development of new technologies and equipment, it is of great importance to minimize environmental pollution. For arc furnaces in the casting shops of manufacturing enterprises, the gas-exhaust system must be improved because the level of toxic emissions within the production buildings exceeds the specifications in environmental standards [1–15]. This is associated with the use of aging and out-of-date equipment [16–21].

As we know, the systems used for the evacuation of gas and dust emissions from arc furnaces of capacity 3–10 t in foundries include trapping hoods, an exhaust line, a fabric filter, an exhaust pump, and a vertical smokestack [22–25].

Inspection of the gas-exhaust systems at various Russian and Ukrainian manufacturing enterprises shows that the air pollution in the production buildings is mainly due to structural shortcomings of the rotary hood above the smelting furnace, which completely covers its roof. In particular, the mobile joint between its housing and the input of the gas-exhaust line is unsatisfactory. The moving joint is not reliably solved by means a flexible sleeve made of thermally stable fabric or a metallic sleeve supporting the hollow cantilever with the hood, which permits rotation relative to the vertical pipe of the exhaust line. That markedly decreases the operational efficiency [26–29].

Accordingly, in the present work, we improve the rotary hood by introducing special gates that prevent the atmospheric emission of the gas–dust mixture at the mobile joints.

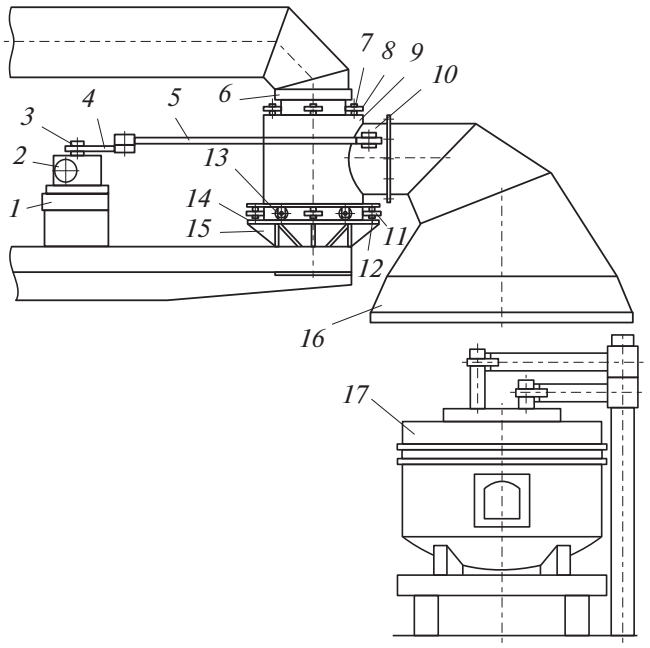

Fig. 1. Hood with rotation mechanism.

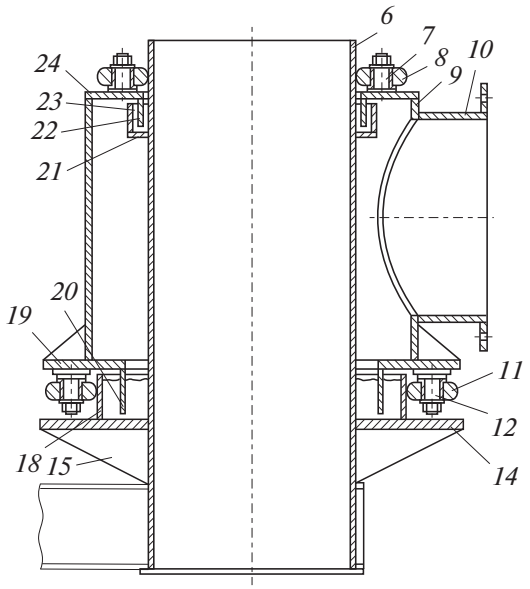

Fig. 2. Sand barriers in rotary hood.

The proposed system for the rotary hood (Fig. 1) is based on design experience for such devices [30–32]. It includes dome *16*, which is coaxially positioned above furnace *17* and attached to hollow cantilever *10*. The dome is able to rotate around the axis of supporting column *6*. A crank system mounted on platform *1* permits 90° rotation of the hood. The platform is maintained at the required height, together with column *6*. The rotation mechanism includes a worm gear drive *2* with a vertical low-speed shaft *3*, to the end of which crank *4* is attached. The crank transmits force to lever *5*, which is hinged to hollow cantilever *10*. The cantilever itself is rigidly connected to sleeve *9*, which covers supporting column *6*. As shown in Fig. 2, the top and bottom of sleeve *9* are equipped, respectively, with flanges *24* and *19*, with cylindrical aprons *22* and *20*, which sit in slots formed by welded flanges *21* and *18*. The flanges seal the seams at supporting column *6* and annular platform *14*, respectively. Both annular chambers are filled with dry sand *23*, which acts as a barrier eliminating both the suction of air into the gas-exhaust channel and the escape of gas and dust from the channel into the atmosphere.

A hole is made in the wall of the supporting column between the flanges, on the furnace side. The shape and size of the hole correspond to the inner cross section of the hollow cantilever *10*. At the upper flange of the sleeve, four vertical shafts *7* with centering rollers *8* are attached at equal distances around the perimeter. The rollers are in contact with the outer surface of supporting column *6*. In turn, four centering rollers *11* are attached analogously to shafts *12* on the lower flange. Between these rollers, four additional vertical rollers *13* support the sleeve on annular platform *14*, by means of gusset *15*, which is rigidly attached to the lower part of supporting column *6*. The presence of rollers *8*, *11*, and *13* at sleeve *9* minimizes the load on the hood-rotation mechanism.

Before designing an industrial prototype of the improved rotary hood, we develop a method of calculating the energy parameters of the hood-rotation mechanism.

In Fig. 3, the total static drag torque M_s on rotation of the sleeve with the hood consists of several components

$$M_s = M_1 + M_2 + M_3 + M_4 + M_5, \quad (1)$$

where M_1 is the drag torque on the rotating sleeve from the upper centering rollers in contact with the outer cylindrical surface of the supporting column; M_2 is the drag torque on the rotating sleeve from the lower centering rollers in contact with the outer cylindrical surface of the lower annular cavity rigidly connected to the supporting column through the annular platform; M_3 is the drag torque on the rotating sleeve from the supporting rollers in contact with the horizontal surface of the annular platform; M_4 and M_5 are frictional torques on the surfaces of the upper and lower annular aprons on rotation in the sand layer.

To calculate the first three components of the static drag torque, which are overcome by the drive in frictional rotation of the hood, we need to first find the reaction in the centering bearings $R_{ce.b}$ and the resultant reaction in the supporting bearing $R_{su.b}$ of the sleeve, on the basis of the equations

$$\sum F_{z_i} = 0; \quad R_{su.b} - G_{sl} - G_d - G_h = 0; \quad (2)$$

$$\sum M_{O_1} = 0; \quad R_{ce.b}h - G_d x_2 - G_h x_3 = 0. \quad (3)$$

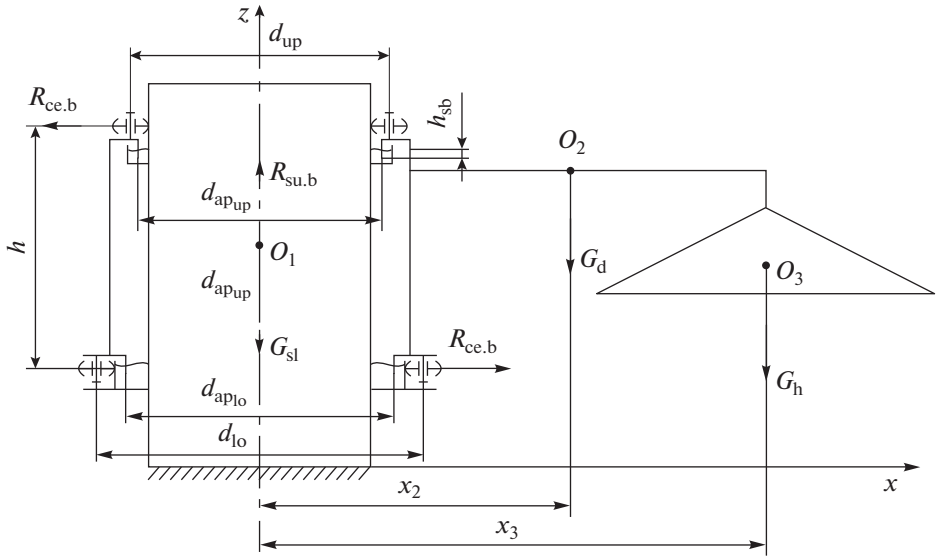

Fig. 3. Rotary drive of gas-capture hood in the exhaust system of a casting-shop arc furnace.

Hence

$$R_{su.b} = G_{sl} + G_d + G_h; \quad R_{ce.b} = \frac{G_d x_2 + G_h x_3}{h}.$$

Then

$$M_1 = R_{ce.b}\left(\frac{\mu d_{ce} + 2k}{D_{ce}}\right)\frac{d_{up}}{2};$$

$$M_2 = R_{ce.b}\left(\frac{\mu d_{ce} + 2k}{D_{ce}}\right)\frac{d_{lo}}{2}.$$

Here μ is the slipping-friction coefficient; d_{ce} is the diameter of the shaft on which the centering rollers are mounted; k is the rolling-friction coefficient; D_{ce} is the external diameter of the centering roller; d_{up} and d_{lo} are the diameters of the circles on which , respectively, the rotational axes of the upper and lower centering rollers lie.

Correspondingly

$$M_3 = R_{su.b}\left(\frac{\mu d_{su} + 2k}{D_{su}}\right)\frac{d_{lo}}{2}.$$

Here d_{su} is the diameter of the shaft on which the supporting roller is mounted; and D_{su} is the external diameter of the supporting roller.

In determining the components M_4 and M_5 of the drag torque on the sleeve, we use Fig. 3, where h_{sb} is the immersion depth of the annular apron in the sand barrier; d_{ap} is the internal diameter of the apron; and δ is its thickness.

The pressure of the column of friable material is

$$P_{fr} = \rho_s g h_{sb}, \quad (4)$$

where ρ_s is the packing density of the sand; and g is the acceleration due to gravity.

The mean pressure acting on the inner and outer surfaces of the annular apron, which are immersed in the sand layer, is

$$P_{me} = 0.5 P_{fr} k_{la}, \quad (5)$$

where k_{la} is the lateral pressure coefficient; $k_{la} = 0.30$–0.35.

The force exerted on the apron wall by the sand is

$$F_w = P_{me}\left[\pi d_{ap} h_{sb} + \pi(d_{ap} + 2\delta) h_{sb}\right]. \quad (6)$$

When the apron rotates in the sang layer, the frictional force that arises is

$$F_{fr} = F_w k_{s.ap}, \quad (7)$$

where $k_{s.ap}$ is the slipping-friction coefficient between the apron surface and the sand layer.

Then the frictional drag torques on the sleeve in the upper and lower annular sand barriers are

$$M_4 = F_{fr}\frac{d_{ap_{up}}}{2}; \quad (8)$$

$$M_5 = F_{fr}\frac{d_{ap_{lo}}}{2}, \quad (9)$$

where $d_{ap_{up}}$ and $d_{ap_{lo}}$ are the diameters of the upper and lower annular aprons.

The dynamic torque in drive startup is

$$M_{dy} = J\varepsilon, \quad (10)$$

where J is the total moment of inertia of the system relative to the z axis; and ε is the angular acceleration of the system during the startup period t_{st}.

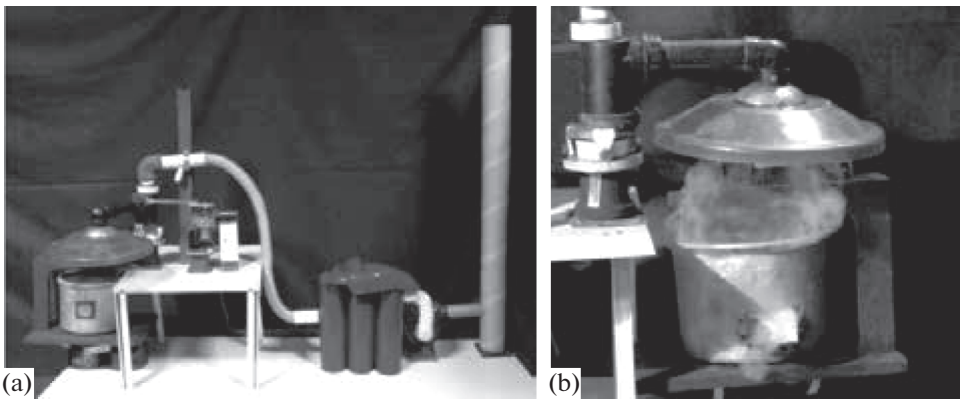

Fig. 4. Model of improved gas-exhaust system for an arc furnace (a) and motion of smoke fluxes from the system during a steel-making simulation (b).

The total moment of inertia of the system relative to the z axis is

$$J = \sum \left(J_{C_i} + m_i x_i^2 \right), \tag{11}$$

where J_{C_i} is the moment of inertia of a structural element in the system relative to an axis passing through its center of mass; m_i is the mass of the structural element; x_i is the distance of the center of gravity of the structural element relative to the z axis.

The angular acceleration of the system is

$$\varepsilon = \frac{\omega}{t_{st}}, \tag{12}$$

where ω is the specified angular velocity of the mobile part of the system, s^{-1}.

The static power of the drive is

$$N_s = \frac{M_s \omega}{\eta_{me}}, \tag{13}$$

where η_{me} is the efficiency of the mechanism.

The total gear ratio of the drive in the hood's rotation mechanism is

$$i_{tot} = i_{lev} i_{gm} = \frac{\omega_{mo}}{\omega}, \tag{14}$$

where i_{lev} is the gear ratio of the lever mechanism; i_{gm} is the gear ratio of the gear–motor unit; and ω_{mo} is the angular velocity of the motor shaft, s^{-1}.

The carrying capacity of the motor selected from the catalog must be verified

$$\frac{M_s + M_{dy}}{M_{ra} i_{tot}} \le \lambda, \tag{15}$$

where M_{ra} and λ are the manufacturer's stated values of the rated torque and the mean starting torque increment of the selected motor.

To verify these proposals and formulas, we conduct laboratory experiments with a 1 : 10 scale model of the system, containing operational physical models of all the structural components in the gas-exhaust system of an 8-t arc furnace (Fig. 4a).

In accordance with the experiment design, we study the variation in the loads on the elements of the lever mechanism in the hood model on motion from the working position to the rest position and back. We also establish the increment in the drag torque on the rotating hood due to the frictional forces on the cylindrical aprons on rotation in the sand layer. The characteristics are monitored by means of a system assembled in accordance with the recommendations in [33]. It includes a tensoresistive converter, an ac amplifier, an analog–digital converter, and a computer with a printer. The tensoresistive converter is a lever transmitting force from the crank to the hollow cantilever. To that end, two 200-Ω foil tensosensors are glued to the plane surface of the lever along the longitudinal symmetry axis. The tensosensors are connected to the amplifier in a half-bridge circuit by means of screening cable. The electrical signal from the half-bridge during extension or compression of the lever under the action of the transmitted force is amplified, converted to digital form, and sent to the computer. Then the signal is analyzed by means of special software, and the recorded load is shown as a function of the time on the monitor screen. This graph may be sent to the printer.

By means of this monitoring system, the longitudinal load on the lever is measured in the absence and presence of the dry sand sealing the moving joint of the supporting column and the covering sleeve, which is rigidly connected to the hollow cantilever at the free end of the hood.

Before interpretation of the signals from the analog–digital converter, we need to calibrate the tensoresistive converter. The readings are analyzed by the statistical method recommended in [34]. Then the calibration curve is plotted, and the error of the measurement method is established. It is no more than 10%.

Table 1. Calculated drive parameters of the hood-rotation mechanism for arc furnaces of capacity 3–10 t

Furnace capacity, t	Basic dimensions of system components, mm					Gravitational force on components, N			Components of the drag torque on the rotating hood, N m					M_s, N m	ω, s^{-1}	N_s, kW
	d_{up}	d_{lo}	h	x_2	x_3	G_{sl}	G_d	G_h	M_1	M_2	M_3	M_4	M_5			
3	800	1000	960	1200	2300	1960	1350	1650	56	70	62	24	31	243	0.5	0.22
5	800	1000	1050	1320	2450	1960	1500	1800	61	76	66	24	31	258	0.5	0.22
8	1000	1300	1200	1500	2600	2940	2200	2500	102	133	124	37	46	442	0.4	0.32
10	1000	1300	1320	1600	2850	2940	2450	2900	115	150	134	37	46	482	0.4	0.32

On the basis of the calibration curve, we conclude that the total drag force due to the friction in the upper and lower sand barriers on hood rotation amounts to 20–26% of the total load on the drive.

Table 1 presents the components of the total static drag torque on sleeve rotation. We see that the total contribution of the frictional torques M_4 and M_5 due to the sand barriers is 17–23% of M_s. Thus, the experimental and calculation results are in satisfactory agreement.

As well as measuring the loads on the components of the model, we make video recordings of the smoke issuing from the model through the gaps between its housing and the roof during simulations of steel production. To that end, smoke is supplied to the working space of the model at low pressure from a special smoke generator. After passing through the discharge channel and gaps formed by the edges of the holes in the roof and the electrodes, the smoke is collected under hood and is then drawn by a suction pump through the exhaust line to a vertical smokestack. Viewing of the videos (including stop-frame examination) shows that all of the smoke escaping from through the gaps is extracted from the working zone (Fig. 4b). No leakage of the smoke is observed at the sand barriers of the rotary hood. In other words, the mobile joints are reliably sealed.

The results of this research have been used in a working design for reconstruction of the gas-exhaust system for an 8-t arc furnace.

CONCLUSIONS

On the basis of our theoretical and experimental results, aging gas-exhaust systems at arc furnaces of capacity 3–10 t in the foundries of manufacturing enterprises may be improved. That will decrease the gas and dust emissions to the working zone in steelmaking.

REFERENCES

1. Eronko, S.P., Gorbatyuk, S.M., Oshovskaya, E.V., and Starodubtsev, B.I., New engineering solutions in creation of mini-BOF for metallic waste recycling, *IOP Conf. Ser.: Mater. Sci. Eng.*, 2018, vol. 287, no. 1, art. ID 012004.
2. Eron'ko, S.P., Gorbatyuk, S.M., Oshovskaya, E.V., and Starodubtsev, B.I., Development of automatic system of gas-dynamic cut-off of slag for converter with rotating vessel shell, *Izv. Vyssh. Uchebn. Zaved., Chern. Metall.*, 2017, vol. 60, no. 11, pp. 863–869.
3. Eron'ko, S.P., Oshovskaya, E.V., and Tkachev, M.Yu., Fast replacement of submersible tundish nozzles in a continuous slab-casting machine, *Steel Transl.*, 2016, vol. 46, no. 1, pp. 33–38.
4. Keropyan, A.M., Kantovich, L.I., Voronin, B.V., Kuziev, D.A., and Zotov, V.V., Influence of uneven distribution of coupling mass on locomotive wheel pairs, its tractive power, straight and curved sections of industrial rail tracks, *IOP Conf. Ser.: Earth Environ. Sci.*, 2017, vol. 87, no. 6, art. ID 062005.
5. Keropyan, A.M. and Gerasimova, A.A., Connection of the temperature in contact area of the wheel-rail system with the railway slope of industrial railway transport, *Izv. Vyssh. Uchebn. Zaved., Chern. Metall.*, 2017, vol. 60, no. 5, pp. 355–363.
6. Bardovskiy, A.D., Gorbatyuk, S.M., Keropyan, A.M., and Bibikov, P.Ya., Assessing parameters of the accelerator disk of a centrifugal mill taking into account features of particle motion on the disk surface, *J. Frict. Wear*, 2018, vol. 39, no. 4, pp. 326–329.
7. Bardovsky, A., Gerasimova, A., and Aydunbekov, A., The principles of the milling equipment improvement, *MATEC Web Conf.*, 2018, vol. 224, art. ID 01019.
8. Gorbatyuk, S., Kondratenko, V., and Sedykh, L., Tool stability analysis for deep hole drilling, *MATEC Web Conf.*, 2018, vol. 224, art. ID 01035.
9. Gerasimova, A., Gorbatyuk, S., and Devyatiarova, V., Application of gas-thermal coatings on low-alloyed steel surfaces, *Solid State Phenom.*, 2018, vol. 284, pp. 1284–1290.
10. Zarapin, A.Yu., Shur, A.I., and Chichenev, N.A., Improvement of the unit for rolling aluminum strip clad with corrosion-resistant steel, *Steel Transl.*, 1999, vol. 29, no. 10, pp. 69–71.
11. Zarapin, A.Yu., Stanishevskii, S.E., and Chichenev, A.N., Continuous line for the production of strips with a gas-thermal coating of nickel alloys, *Tyazh. Mashinostr.*, 1999, no. 6, pp. 16–20.
12. Zarapin, A.Yu. and Chichenev, A.N., Design of lines for the production of composite materials based on the object-oriented approach, *Tyazh. Mashinostr.*, 1999, no. 6, pp. 21–25.

13. Gorbatyuk, S.M., Gerasimova, A.A., and Belkina, N.N., Applying thermal coatings to narrow walls of the continuous-casting molds, *Mater. Sci. Forum*, 2016, vol. 870, pp. 564–567.
14. Pimenov, G.A., Kostyukov, G.A., Ryabov, V.D., and Kobelev, O.A., Production of large-sized solid-forged blanks, *Tyazh. Mashinostr.*, 1991, no. 9, pp. 21–24.
15. Kobelev, O.A., Tsepin, M.A., Skripalenko, M.M., and Popov, V.A., Features of technological layout of manufacture of unique mono-block large-dimension plates, *Adv. Mater. Res.*, 2009, vol. 59, pp. 71–75.
16. Stalinskii, D.V., Pirogov, A.Yu., Shvets, M.N., et al., Gas cleaning of low-tonnage electric steel-smelting furnaces in the foundry, *Metall. Gornorudn. Prom-st'.*, 2016, no. 6, pp. 100–105.
17. Rakhmetova, E.R., Development of a system for cleaning exhaust gases from electric arc furnaces of the foundry shop and measures to improve the environmental friendliness of production, *Materialy Vserossiiskogo forums nauchnoi molodezhi "Bogatstvo Rossii"* (Proc. All-Russ. Forum of Young Scientists "The Wealth of Russia"), Moscow: Mosk. Gos. Tekh. Univ. im. N.E. Baumana, 2018, pp. 275–276.
18. Pavlovich, L.B., Sadykhova, V.V., and Shul'disheva, D.A., Environmental risk assessment of foundry emissions into the atmosphere, *Vestn. Sib. Gos. Ind. Univ.*, 2014, no. 4 (10), pp. 52–55.
19. Rechkalov, A.V., Zinurov, I.Yu., Kuz'min, M.G., et al., Basic requirements to the arc furnaces smelting metal for casting, *Elektrometallurgiya*, 2014, no. 11, pp. 2–5.
20. Malinovskiy, V.S., Technical-economical results of industrial realization of direct current arc furnaces of new generation, *CIS Iron Steel Rev.*, 2014, no. 9, pp. 4–19.
21. Krutyanskii, M.M., Nekhamin, S.M., and Rebikov, E.M., Calculation of gas release from DC and AC arc furnaces in a foundry, *Elektrometallurgiya*, 2016, no. 7, pp. 27–34.
22. Ladygichev, M.G. and Chizhikova, V.M., *Syr'e dlya chernoi metallurgii: Spravochnoe izdanie. Tom 2. Ekologiya metallurgicheskogo proizvodstva* (Raw Materials for Ferrous Metallurgy: Handbook, Vol. 2: Ecology of Metallurgical Industry), Moscow: Teplotekhnik, 2005.
23. Krutyanskii, M.M., Nekhamin, S.M., and Rebikov, E.M., Calculation of gas release from DC and AC arc furnaces in a foundry, *Russ. Metall. (Moscow)*, 2016, vol. 2016, no. 12, pp. 1119–1124.
24. Barkan, M.S. and Kovshov, V.P., Calculation of harmful impurities formation and the technology of cupola dust-and-gas emission intensive cyclone cleaning from solids and gaseous components, *Global J. Pure Appl. Mathem.*, 2016, vol. 12, no. 3, pp. 2323–2333.
25. Gudim, Yu.A., Zinurov, I.Yu., Kiselev, A.D., et al., Rational methods for the intensification of melting in modern arc steel-melting furnaces, *Russ. Metall. (Moscow)*, 2008, vol. 2008, no. 8, pp. 651–654.
26. Malyarov, A.I., *Pechi liteinykh tsekhov* (Foundry Furnaces), Moscow: Mashinostroenie, 2014.
27. Solov'ev, V.P., Gladyshev, S.A., and Vorontsov, V.I., *Proektirovanie novykh i rekonstruktsiya deistvuyushchikh liteinykh tsekhov: uchebnoe posobie* (Design of New and Reconstruction of Existing Foundries: Manual), Moscow: Mosk. Inst. Stali Splavov, 2004.
28. Elizarov, K.A., Krutyanskii, M.M., Nekhamin, I.S., et al., New trends in the development of DC arc furnaces, *Russ. Metall. (Moscow)*, 2014, vol. 2014, no. 6, pp. 443–448.
29. Drobit'ko, M.Yu., Boldin, A.N., Yakovlev, A.I., et al., *Sistemy ochistki otkhodyashchikh gazov plavki i ikh ispol'zovanie v liteinom proizvodstve* (Cleaning Systems for Smelting Gases and Their Use in the Foundry Industry), Moscow: Mashinostroenie, 2004.
30. Artiukh, V., Mazur, V., and Prakash, R., Increasing hot rolling mass of steel sheet products, *Solid State Phenom.*, 2016, vol. 871, pp. 3–8.
31. Artiukh, V., Mazur, V., and Adamtsevich, A., Priority influence of horizontal forces at rolling on operation of main sheet rolling equipment, *MATEC Web Conf.*, 2017, vol. 106, art. ID 04001.
32. Artiukh, V., Mazur, V., and Pokrovskaya, E., Influence of strip bite time in work rolls gap on dynamic loads in strip rolling stands, *MATEC Web Conf.*, 2016, vol. 86, art. ID 01030.
33. Mekheda, V.A., *Tenzometricheskii metod izmereniya deformatsii: uchebnoe posobie* (Strain Gauge Method of Deformations Measuring: Manual), Samara: Samar. Gos. Aerokosm. Univ., 2011.
34. Boltyan, A.V. and Gorobets, I.A., *Teoriya inzhenernykh issledovanii* (Theory of Engineering Research), Sevastopol: Veber, 2001.

Translated by Bernard Gilbert

SPELL: 1. ok